Time-Delayed Feedback Control of Piezoelectric Elastic Beams under Superharmonic and Subharmonic Excitations

Jian Peng [1,2,*], **Mingjiao Xiang** [1], **Luxin Li** [1,3], **Hongxin Sun** [1,2,*] **and Xiuyong Wang** [2]

1   School of Civil Engineering, Hunan University of Science and Technology, Xiangtan 411201, China;
    xmj19941015@163.com (M.X.); DLXIN@mail.dlut.edu.cn (L.L.)
2   Hunan Provincial Key Laboratory of Structures for Wind Resistance and Vibration Control,
    Hunan University of Science and Technology, Xiangtan 411201, China; xywang_cs@sina.com
3   Department of Engineering Mechanics, State Key Laboratory of Structural Analysis for
    Industrial Equipment, Dalian University of Technology, Dalian 116023, China
*   Correspondence: pengjian@hnu.edu.cn (J.P.); cehxsun@hnust.edu.cn (H.S.)

check for
updates

Abstract: The time-delayed displacement feedback control is provided to restrain the superharmonic and subharmonic response of the elastic support beams. The nonlinear equations of the controlled elastic beam are obtained with the help of the Euler–Bernoulli beam principle and time-delayed feedback control strategy. Based on Galerkin method, the discrete nonlinear time-delayed equations are derived. Using the multiscale method, the first-order approximate solutions and stability conditions of three superharmonic and 1/3 subharmonic resonance response on controlled beams are derived. The influence of time-delayed parameters and control gain are obtained. The results show that the time-delayed displacement feedback control can effectively suppress the superharmonic and subharmonic resonance response. Selecting reasonably the time-delayed quantity and control gain can avoid the resonance region and unstable multi-solutions and improve the efficiency of the vibration control. Furthermore, with the purpose of suppressing the amplitude peak and governing the resonance stability, appropriate feedback gain and time delay are derived.

Keywords: piezoelectric elastic beam; time-delayed feedback; superharmonic response; subharmonic response

1. Introduction

The elastic beams have wide application in many engineering fields. Therefore, it is important to investigate the vibration problem of the elastic beams. As a very important topic in structural dynamics, the dynamics problem of the elastic beam is of practical importance in civil engineering [1–3]. At the same time, the vibration control problem of flexible structures has also received extensive attention. Different vibration control strategies are used to study vortex-induced vibrations of a bridge deck [4–6], building structure [7–12], and other structures [13–15]. It is worth mentioning that scholars have carried out much research on piezoelectric-based vibration control [16–26].

As a control strategy, the time-delayed feedback control technology, along with the rapid development of control theory [27–29], sensor testing technology, and computer technology, has attracted widespread attention and practical application in the field of aerospace engineering [30], vehicles engineering [31], mechanical engineering [32], civil engineering [33], etc. Delay feedback control can improve the stability of the controlled system. Based on the time-delayed displacement feedback, the time-delayed velocity feedback and the time-delayed acceleration feedback control strategy, the vibration absorber has excellent effectiveness to suppress the vibration of the system.

In the past few years, the time-delayed feedback control technology has received much attention. An optimal control method for seismic-excited building structures with multiple time delays is investigated [34]. The time delay may be used to improve the system stability [35,36]. The delayed position-feedback technique is used to reduce the payload pendulations [37]. Daqaq et al. [38] presented a comprehensive investigation of the effect of feedback delays on the non-linear vibrations of a piezoelectrically-actuated cantilever beam. Qian and Tang [39] studied the time delay control and presented that it can achieve good control performance of a dynamic beam structure system. Xu and Pu [40] investigated the bifurcations due to time delay in the feedback control system with excitation. Kalmar-Nagy, Stepan, and Moon [41] studied the existence of a subcritical Hopf bifurcation in the delay-differential equation model of the so-called regenerative machine tool vibration. Peng et al. [42] investigated the stability and bifurcation of an SDOFsystem with time-delayed feedback. Li et al. [43] investigated the nonlinear dynamics of a Duffing–van der Pol oscillator under linear-plus-nonlinear state feedback control with a time delay. Kammer and Olgac [29] conceived of a concept study that explores new directions to enhance the performance of such energy-harvesting devices from base excitation. Jin and Hu [44] investigated the stabilization of traffic flow in an optimal velocity model via delayed-feedback control. Omidi and Mahmoodi [45,46] investigated nonlinear vibration suppression of flexible structures using the nonlinear modified positive position feedback approach. El-Ganaini et al. [47] investigated the positive position feedback (PPF) controller for suppression of nonlinear system vibration. Warminski et al. [48] selected control algorithms for active suppression of nonlinear composite beam vibrations. Belhaq et al. [49,50] investigated energy harvesting in a Mathieu–van der Pol–Duffing MEMS device using time delay and quasi-periodic vibrations in a delayed van der Pol oscillator with time-periodic delay amplitude. Ji et al. [51–53] presented modeling and tuning for a time-delayed vibration absorber with friction and investigated sub-harmonic resonances and periodic and chaotic motion of a time-delayed nonlinear system.

These results show that the new control method (time-delayed feedback control) makes the system more stable and improves the control performance. Therefore, in this paper, adopting the time-delayed displacement feedback control strategy, the piezoelectric coupling elastic beam is controlled in order to study its superharmonic resonance and subharmonic resonance response. Based on the established delay dynamic system, we obtained the first-order resonance response approximate solution and analyzed the influence of the control gain and the time delay values on the two resonant responses. We organize the rest of the paper as follows: In Section 2, we present a mathematical formulation of the problem. In Section 3 and Section 4, the three superharmonic resonance and 1/3 subharmonic resonance are respectively discussed by using the method of multiple scales. A short summary of the results is presented in Section 5.

2. Equations of Motion

The mathematical model for the cantilever is based on the nonlinear Euler–Bernoulli beam theory.The partial-differential equation of planar motion and that associated with an external excited elastic beam are as follows [54]:

$$m\ddot{v} + c\dot{v} - EAp(t)v'' + EIv'''' + kv\delta(x-l) - \frac{EA}{2l}v''\int_0^l v'^2 dx = q(x,t) + F_n(x)\cos\Omega t, \qquad (1)$$

$$v(0,t) = 0, v'(0,t) = 0, v''(l,t) = 0, EIv'''(l,t) + kv(l,t) = 0, \qquad (2)$$

where m is the linear density; c is the coefficient of linear viscous damping per unit length; v denotes the displacement component along the y-axis; the primes and overdots indicate the derivatives with respect to the arc length x and time t, respectively; E is Young's modulus of elasticity; A is the cross-sectional area; I is the moment of inertia about the neutral axis of the beam; l is the length of the

beam; and $p(t)$ is the axial force; The distributed load $q(x,t)$ of the piezoelectric actuator (see Figure 1), is given by:

$$q(x,t) = \frac{\partial^2 M}{\partial x^2},$$

(3)

where M is a uniformly-distributed bending moment expressed as:

$$M = \frac{3bdd_{31}E_aEIV_a(t)}{3EI + 6bE_at_ad^2 + 2bE_at_a^3}[H(x - x_1) - H(x - x_2)].$$

(4)

where b and t_a are the width and thickness of the piezoelectric actuator, respectively; d_{31} is a piezoelectric constant; E_a is the actuator Young's modulus; t_b is the thickness of the beam; $V_a(t)$ is the control voltage; $H(x)$ is the Heaviside step function; and x_1 and x_2 are the starting and ending coordinates of the piezoelectric strip.
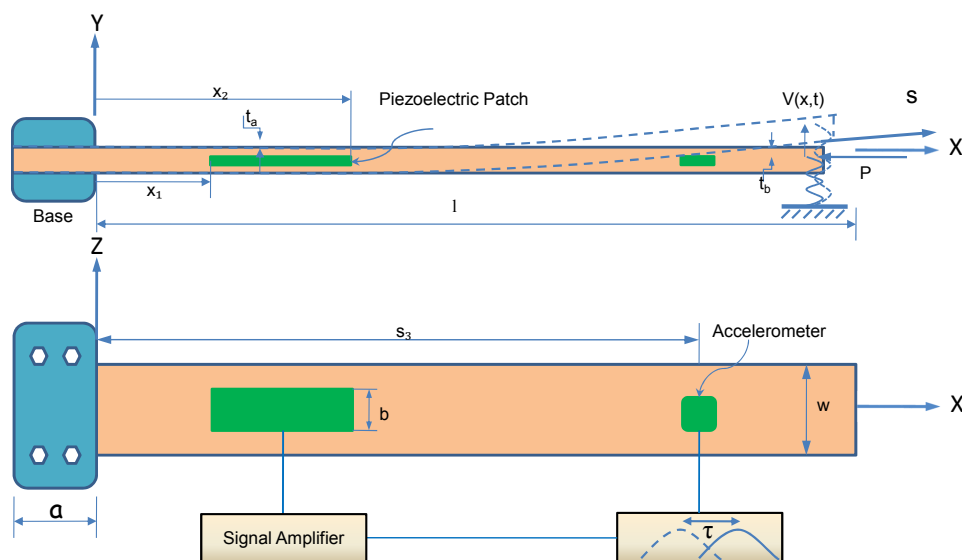

Figure 1. The theory model of the controlled beams.

In this paper, the time delayed feedback control is used to suppress the large vibration of the beam. The block diagram is shown in Figure 2.
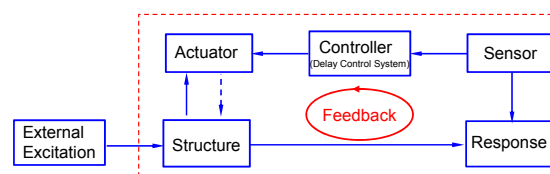

Figure 2. A block diagram of the time-delayed feedback control.

We derive a reduced-model for the system under consideration by using the Galerkin procedure in the form:

$$v = \sum_{i=1}^{\infty} \phi_i(x)q_i(t),$$

(5)

where the $q_i(t)$ are generalized temporal coordinates and the $\phi_i(x)$ are the linear mode shapes of a elastic beams and are given by:

$$\phi_i(x) = A_i\left[\cos\delta_ix - \cosh\varepsilon_ix - \sigma_i\left(\sin\delta_ix - \frac{\delta_i}{\varepsilon_i}\sinh\varepsilon_ix\right)\right]$$

(6)

where:

$$\sigma_i = \frac{\delta_i^2 \cos \delta_i l + \varepsilon_i^2 \cosh \varepsilon_i l}{\delta_i^2 \sin \delta_i l + \varepsilon_i \delta_i \sinh \varepsilon_i l}, \delta_i = \sqrt{\left(r_i + \frac{g^4}{4}\right)^{1/2} + \frac{g^2}{4}}, \varepsilon_i = \sqrt{\left(r_i + \frac{g^4}{4}\right)^{1/2} - \frac{g^2}{4}},$$

and $g^2 = p(t)/EI$, while r_i is calculated using the following transcendental equation:

$$\begin{aligned}
EI\delta_i^5 + EI\varepsilon_i^4 \delta_i + 2EI\varepsilon_i^2 \delta_i^3 \cos \delta_i l \cosh \varepsilon_i l + EI(\varepsilon_i \delta_i^4 - \varepsilon_i^3 \delta_i^2) \sin \delta_i l \sinh \varepsilon_i \\
-k(\varepsilon_i^2 + \delta_i^2) \sin \delta_i l \sinh \varepsilon_i l + k(\delta_i^3/\varepsilon_i + \varepsilon_i \delta_i) \cos \delta_i l \sinh \varepsilon_i = 0
\end{aligned} \tag{7}$$

Substituting Equation (5) into Equation (1) and using the Galerkin method, we obtain the following set of nonlinear ordinary differential equations:

$$\ddot{q}_n(t) + \mu_n \dot{q}_n(t) + \omega_n^2 q_n(t) + \sum_{i,j,k=1}^{\infty} \Gamma_{nijk} q_i(t) q_j(t) q_k(t)$$

$$= M_n V_a(t) + f_n(x) \cos \Omega t, \quad n = 1, 2, ..., \infty, \tag{8}$$

where:

$$\begin{aligned}
\mu_n &= \frac{c}{m}, \quad \Gamma_{nijk} = -\frac{EA}{2ml} \int_0^l \phi_i''(x) \phi_n(x) \int_0^l \phi_j'(x) \phi_k'(x) dx dx, \\
M &= \frac{3bdd_{31}E_aEI}{3EI + 6bE_a t_a d^2 + 2bE_a t_a^3} [\phi(x_1) - \phi(x_2)], \quad f_n = F_n \sum_0^{\infty} \phi_n dx.
\end{aligned} \tag{9}$$

We nondimensionalize Equation (8) and obtain:

$$\ddot{q}_n^*(t^*) + \mu_n^* \dot{q}_n^*(t) + \omega_n^* 2 q_n^*(t^*) + \sum_{i,j,k=1}^{\infty} \Gamma_{nijk}^* q_i^*(t^*) q_j^*(t^*) q_k^*(t^*)$$

$$= M_n^* V_a^*(t^*) + f_n^* \cos \Omega^* t^*, \quad n = 1, 2, ..., \infty, \tag{10}$$

where $t^* = \omega_1 t, \tau^* = \omega_1 \tau, q_n^* = q_n(t)/l, \omega_n^* = \omega_n/\omega_1, \mu_n^* = \mu_n/\omega_1, \Gamma_{nijk}^* = \Gamma_{nijk} l^2/\omega_1^2, M_n^* = M_n, f_n^* = f/\omega_1 l$, and $\Omega^* = \Omega/\omega_1$. For convenience, remove the asterisk of the following equation.

In this article, the driving voltage of piezoelectric excitation uses the time-delayed displacement feedback strategy, for the following form:

$$V_a(t) = \sum_{m=1}^{\infty} -\bar{k}_a \phi_m(x_3) q_m(t - \tau), \tag{11}$$

where $\bar{k}_a$ is control gain and τ is time delay. Substituting $V_a(t)$ into Equation (10), we obtain:

$$\ddot{q}_n(t) + \mu_n \dot{q}_n(t) + \omega_n^2 q_n(t) + \sum_{i,j,k=1}^{\infty} \Gamma_{nijk} q_i(t) q_j(t) q_k(t) = -\sum_{m=1}^{\infty} k_{anm} q_m(t - \tau) + f_n \cos \Omega t, \tag{12}$$

where $M_n \bar{k}_a \phi_m(x_3) = k_{anm}$.

The governing equation expressed in the modal coordinate form is:

$$\ddot{q}_n(t) + \mu_n \dot{q}_n(t) + \omega_n^2 q_n(t) + \Gamma_{nnnn} q_n^3(t) = -k_{ann} q_n(t - \tau) + f_n \cos \Omega t. \tag{13}$$

3. Superharmonic Resonance

We use the method of multiple scales [55–57] to solve three superharmonic resonance. The adjusting parameters are as follows: $\mu_n = O(\varepsilon), \Gamma_{nnnn} = O(\varepsilon), k_{ann} = O(\varepsilon), f_n = O(\varepsilon), 3\Omega = \omega_0 + \varepsilon\sigma, \sigma = O(1)$. We express the solution of Equation (13) in the form:

$$q_n(t;\varepsilon) = q_{n0}(T_0, T_1, ...) + \varepsilon q_{n1}(T_0, T_1, ...) + ..., \tag{14}$$

Substituting Equation (14) into Equation (13) and equating the coefficients of ε^0 and ε^1 on both sides, we obtain:

$$D_0^2 q_{n0} + \omega_0^2 q_{n0} = f_n \cos \Omega T_0, \tag{15}$$

$$D_0^2 q_{n1} + \omega_0^2 q_{n1} = -2D_0 D_1 q_{n0} - \mu_n D_0 q_{n0} - \Gamma_{nnnn} q_{n0}^3 - k_{ann} q_{n0}(t - \tau). \tag{16}$$

The general solution of Equation (15) can be written as:

$$q_{n0} = A_n(T_1) \exp(i\omega_0 T_0) + \Lambda_n \exp(i\Omega T_0) + cc, \tag{17}$$

where $i = \sqrt{-1}, \Lambda_n = \frac{1}{2} f_n (\omega_0^2 - \Omega^2)^{-1}$, and cc stands for the complex conjugate of the preceding terms. Substituting q_{n0} into Equation (16), we obtain:

$$
\begin{aligned}
D_0^2 q_{n1} + \omega_0^2 q_{n1} = & - [i\omega_0(2A_n' + \mu_n A_n) + 6\Gamma_{nnnn} A_n \Lambda_n^2 + 3\Gamma_{nnnn} A_n^2 \bar{A}_n \\
& + k_{ann} A_n \exp(-i\omega_0 \tau)] \exp(i\omega_0 T_0) - \Gamma_{nnnn} A_n^3 \exp(3i\omega T_0) \\
& + \Gamma_{nnnn} \Lambda_n^3 \exp(3i\Omega T_0) + 3\Gamma_{nnnn} A_n^2 \Lambda_n \exp[i(2\omega_0 + \Omega)T_0] \\
& + 3\Gamma_{nnnn} \bar{A}_n^2 \Lambda_n \exp[i(\Omega - 2\omega_0)T_0] + 3\Gamma_{nnnn} A_n \Lambda_n^2 \exp[i(\omega_0 + 2\Omega)T_0] \\
& + 3\Gamma_{nnnn} A_n \Lambda_n^2 \exp[i(\omega_0 - 2\Omega)T_0] - \Lambda_n[i\mu_n \Omega + 3\Gamma_{nnnn}\Lambda_n^2 + 6\Gamma A_n \bar{A}_n] \\
& \exp(i\Omega T_0) - k_{ann} \Lambda_n \exp[i\omega_0(T_0 - \tau)] + cc.
\end{aligned}
\tag{18}
$$

Secular terms will be eliminated from the particular solution of Equation (18), if we let:

$$
\begin{aligned}
i\omega_0(2A_n' + \mu_n A_n) + 6\Gamma_{nnnn} A_n \Lambda_n^2 + 3\Gamma_{nnnn} A_n^2 \bar{A}_n + \Gamma_{nnnn} \Lambda_n^3 \exp(i\sigma T_1) \\
+ k_{ann} A_n \exp(-i\omega_0 \tau) = 0.
\end{aligned}
\tag{19}
$$

To solve Equation (19), we write A_n in the polar form:

$$A_n = \frac{1}{2} a_n \exp(i\beta_n), \tag{20}$$

where a_n and β_n are real functions of T_1. Substituting Equation (20) into Equation (19) and separating the result into real and imaginary parts, we have:

$$a_n' = -\frac{1}{2}\mu_{ne} a_n - \frac{\Gamma_{nnnn}\Lambda_n^3}{\omega_0} \sin \gamma_n, \tag{21}$$

$$a_n \gamma_n' = \sigma_e a_n - \frac{3\Gamma_{nnnn}\Lambda_n^2}{\omega_0} a_n - \frac{3\Gamma_{nnnn}}{8\omega_0} a_n^3 - \frac{\Gamma_{nnnn}\Lambda_n^3}{\omega_0} \cos \gamma_n, \tag{22}$$

where $\gamma_n = \sigma T_1 - \beta_n, \mu_{ne} = \mu_n - k_{ann} \sin(\omega_0 \tau)/\omega_0$ and $\sigma_e = \sigma - k_{ann} \cos(\omega_0 \tau)/(2\omega_0)$. Therefore, for the first approximation:

$$q_n = \frac{1}{2} a_n \cos(3\Omega t - \gamma_n) + f_n(\omega_0^2 - \Omega^2)^{-1} \cos \Omega t + O(\varepsilon). \tag{23}$$

where a_n and γ_n are defined by Equations (21) and (22).

The steady-state motions correspond to $a_n' = \gamma_n' = 0$; that is, they correspond to the solutions of:

$$-\frac{1}{2}\mu_n a_n + \frac{k_{ann}a_n}{2\omega_0}\sin(\omega_0\tau) = \frac{\Gamma_{nnnn}\Lambda_n^3}{\omega_0}\sin\gamma_n \tag{24}$$

$$\left(\sigma - \frac{3\Gamma_{nnnn}\Lambda_n^2}{\omega_0}\right)a_n - \frac{3\Gamma_{nnnn}}{8\omega_0}a_n^3 - \frac{k_{ann}a_n}{2\omega_0}\cos(\omega_0\tau) = \frac{\Gamma_{nnnn}\Lambda_n^3}{\omega_0}\cos\gamma_n \tag{25}$$

Squaring and adding these equations leads to the frequency-response equation:

$$\left[\left(-\frac{1}{2}\mu_n + \frac{k_{ann}}{2\omega_0}\sin(\omega_0\tau)\right)^2 + \left(\sigma - \frac{3\Gamma_{nnnn}\Lambda_n^2}{\omega_0} - \frac{3\Gamma_{nnnn}}{8\omega_0}a_n^2 - \frac{k_{ann}}{2\omega_0}\cos(\omega_0\tau)\right)^2\right]a_n^2$$
$$= \frac{\Gamma_{nnnn}^2\Lambda_n^6}{\omega_0^2}. \tag{26}$$

Here, we study the stability of the steady-state motion , setting:

$$a = a_{n0} + a_{n1}, \gamma_n = \gamma_{n0} + \gamma_{n1}, \tag{27}$$

Substituting Equation (27) into Equations (21) and (22), expanding for small a_{n1} and γ_{n1}, noting that a_{n0} and γ_{n0} satisfy Equation (24), and keeping linear terms in a_{n1} and γ_{n1}, we obtain:

$$a_{n1}' = -\frac{1}{2}\mu_{ne}a_{n1} - a_{n0}(\sigma_e - \frac{3\Gamma_{nnnn}\Lambda_n^2}{\omega_0} - \frac{3\Gamma_{nnnn}a_{n0}^2}{8\omega_0})\gamma_{n1}, \tag{28}$$

$$(1 + \frac{a_{n1}}{a_{n0}})\gamma_{n1}' = \frac{1}{a_{n0}}(\sigma_e - \frac{3\Gamma_{nnnn}\Lambda_n^2}{\omega_0} - \frac{9\Gamma_{nnnn}}{8\omega_0}a_{n0}^2)a_{n1} - \frac{1}{2}\mu_{ne}\gamma_{n1}, \tag{29}$$

Using Equations (28) and (29), one can obtain the following eigenvalue equation:

$$\begin{vmatrix} -\frac{1}{2}\mu_{ne} - \lambda & -a_{n0}(\sigma_e - \frac{3\Gamma_{nnnn}\Lambda_n^2}{\omega_0} - \frac{3\Gamma_{nnnn}a_{n0}^2}{8\omega_0}) \\ \frac{1}{a_{n0}}(\sigma_e - \frac{3\Gamma_{nnnn}\Lambda_n^2}{\omega_0} - \frac{9\Gamma_{nnnn}}{8\omega_0}a_{n0}^2) & -\frac{1}{2}\mu_{ne} - \lambda \end{vmatrix} = 0$$

Expanding this determinant yields:

$$\lambda^2 + \mu_{ne}\lambda + \rho = 0, \tag{30}$$

where:

$$\rho = \frac{1}{4}\mu_{ne}^2 + (\sigma_e - \frac{3\Gamma_{nnnn}\Lambda_n^2}{\omega_0} - \frac{3\Gamma_{nnnn}a_{n0}^2}{8\omega_0})(\sigma_e - \frac{3\Gamma_{nnnn}\Lambda_n^2}{\omega_0} - \frac{9\Gamma_{nnnn}}{8\omega_0}a_{n0}^2).$$

Hence, the steady-state motions are stable when $\mu_{ne} > 0$ and $\rho > 0$, and are otherwise unstable.

Through concrete examples, we carry out the numerical analysis and discussion of the superharmonic resonance response of the first order modal of the controlled beam. Geometric dimensions and material characteristic parameters of the beam and piezoelectric actuator are as follows. Beam: $l = 99.62 \times 10^{-2}$ m, $A = 15.36 \times 10^{-4}$ m^2, $E = 34.5$ GPa, $I = 9.8662 \times 10^{-8}$ m^4, $k = 6.872 \times 10^4$ N/m, $p = 2.574 \times 10^{-1}$ kN, $m = 4.4$ kg/m. Piezoelectric actuator: $d_{31} = -270 \times 10^{-12}$ m/V, $E_a = 108$ GPa, $b = 0.2 \times 10^{-2}$ m, $2t_a = 0.04 \times 10^{-2}$ m, $d = 0.5 \times 10^{-2}$ m, $x_1 = 12 \times 10^{-2}$ m, $x_2 = 18 \times 10^{-2}$ m, $x_3 = 80 \times 10^{-2}$ m. For such an elastic beam, the first four non-dimensional natural frequencies and eigenfunctions are shown in Figure 3.
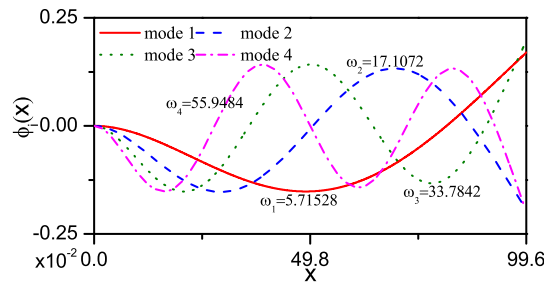
Figure 3. The planar mode shapes and natural frequencies of the elastic beam.

In order to more intuitively display the suppression effect of the delay feedback control, Figure 4a shows the response of the system with no control, active control, and time delay feedback control. It shows that the time delay feedback control can achieve significant vibration suppression effects, and the effect is better than active control. On the other hand, the delay feedback control depends on two important parameters, the control gain and the time lag value. If the parameters are not properly selected, the system response will increase, as shown in Figure 4b.

Figure 4. Time history curve of the system response. (**a**) Time history curve under no control, active control, and time delay feedback control; (**b**) increased response under time delay feedback control.

Given $f_1 = 0.005$, $u_1 = 0.02$, Figure 5 is the amplitude frequency curve of the first order modal of the beam with different control gain and time delay, from which we can see, when $k_{a11} = 0$, the non-control system response amplitude is larger. When $k_{a11} \neq 0$, that is the response amplitude is evidently suppressed by using the time-delayed displacement feedback control. In particular, when $\tau = \pi/2$, $k_{a11} = 0.5$, the peak amplitude of the response of the beam is decreased by about 53%, which is compared with $\tau = \pi/2$, $k_{a11} = 0.25$. Moreover, the curves are multivalued. The multivalued of the response curve due to the nonlinearity has significance from the physical point of view because it leads to jump phenomena.

Figure 6 shows the first order modal excitation-response amplitude curve of the controlled beam in the case of different time delay τ and detuning parameter σ. We can see that as the delay time increases, the response amplitude increases. At the same time, it also can be demonstrated by Figure 7. Figure 7 shows the time history curve of the system response when $\tau = \pi/4$ and $\tau = \pi/2$.
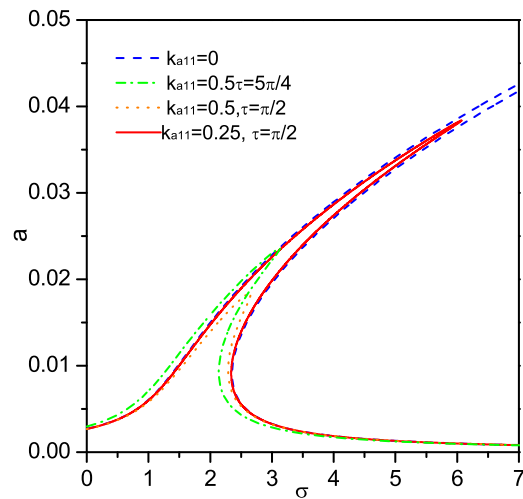
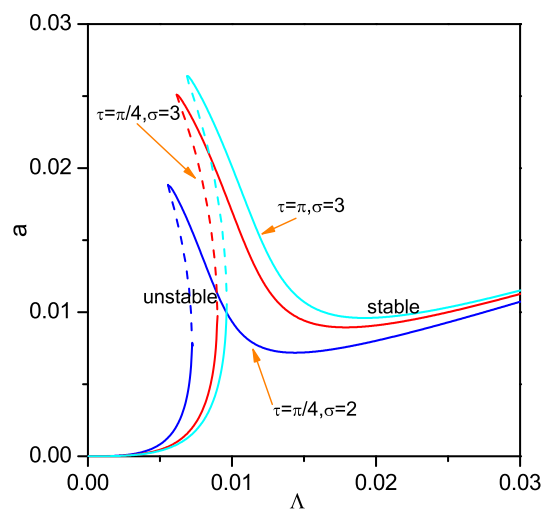**Figure 5.** The amplitude-frequency curve of the superharmonic resonance.

Figure 6. The response-excitation amplitude curve of the superharmonic resonance.
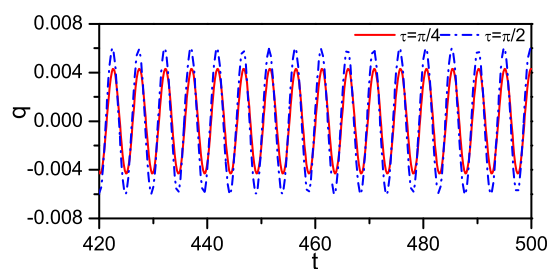

Figure 7. The time history curves of the response of the controlled beams.

4. 1/3 Subharmonic Resonance

In this section, to analyze the 1/3 subharmonic resonance of the system , we let:

$$\Omega = 3\omega_0 + \varepsilon\sigma. \tag{31}$$

To eliminate the secular terms in Equation (18), we put:

$$i\omega_0(2A'_n + \mu_n A_n) + 6\Gamma_{nnnn}A_n\Lambda_n^2 + 3\Gamma_{nnnn}A_n^2\bar{A}_n + 3\Gamma_{nnnn}\Lambda_n\bar{A}_n^2\exp(i\sigma T_1)$$
$$+k_{ann}A_n\exp(-i\omega_0\tau) = 0, \tag{32}$$

Substituting $A_n = a_n\exp(i\beta_n)/2$ into Equation (32) and separating the result into real and imaginary parts, we have:

$$a'_n = -\mu_{ne}a_n - \frac{3\Gamma_{nnnn}\Lambda_n}{4\omega_0}a_n^2\sin\gamma_n, \tag{33}$$

$$a_n\gamma'_n = \left(\sigma_e - \frac{9\Gamma_{nnnn}\Lambda_n^2}{\omega_0}\right)a_n - \frac{9\Gamma_{nnnn}}{8\omega_0}a_n^3 - \frac{9\Gamma_{nnnn}\Lambda_n}{4\omega_0}a_n^2\cos\gamma_n, \tag{34}$$

where $\gamma_n = \sigma T_1 - \beta_n$, $\mu_{ne} = \mu_n/2 - k_{ann}\sin(\omega_0\tau)/(2\omega_0)$ and $\sigma_e = \sigma - 3k_{ann}\cos(\omega_0\tau)/(2\omega_0)$. Therefore, for the first approximation:

$$q_n = \frac{1}{2}a_n\cos[\frac{1}{3}(\Omega t - \gamma_n)] + f_n(\omega_0^2 - \Omega^2)^{-1}\cos\Omega t + O(\varepsilon). \tag{35}$$

The steady-state motions correspond to $a'_n = \gamma'_n = 0$, that is they correspond to the solutions of:

$$-\mu_{ne}a_n = \frac{3\Gamma_{nnnn}\Lambda_n}{4\omega_0}a_n^2\sin\gamma_n \tag{36}$$

$$\left(\sigma_e - \frac{9\Gamma_{nnnn}\Lambda_n^2}{\omega_0}\right)a_n - \frac{9\Gamma_{nnnn}}{8\omega_0}a_n^3 = \frac{9\Gamma_{nnnn}\Lambda_n}{4\omega_0}a_n^2\cos\gamma_n \tag{37}$$

Squaring and adding these equations leads to the frequency-response equation:

$$\left[9\mu_{ne}^2 + \left(\sigma_e - \frac{9\Gamma_{nnnn}\Lambda_n^2}{\omega_0} - \frac{9\Gamma_{nnnn}}{8\omega_0}a_n^2\right)^2\right]a_n^2 = \frac{81\Gamma_{nnnn}^2\Lambda_n^2}{16\omega_0^2}a_n^4. \tag{38}$$

Equation (38) shows that either $a_n = 0$ or:

$$9\mu_{ne}^2 + \left(\sigma_e - \frac{9\Gamma_{nnnn}\Lambda_n^2}{\omega_0} - \frac{9\Gamma_{nnnn}}{8\omega_0}a_n^2\right)^2 = \frac{81\Gamma_{nnnn}^2\Lambda_n^2}{16\omega_0^2}a_n^2, \tag{39}$$

which is quadratic in a_n^2. Its solution is:

$$a_n^2 = \nu \pm (\nu^2 - \iota)^{1/2}, \tag{40}$$

where:

$$\nu = \frac{8\omega_0\sigma_e}{9\Gamma_{nnnn}} - 6\Lambda_n^2 \quad \text{and} \quad \iota = \frac{64\omega_0^2}{81\Gamma_{nnnn}^2}\left[9\mu_{ne}^2 + \left(\sigma_e - \frac{9\Gamma_{nnnn}\Lambda_n^2}{\omega_0}\right)^2\right], \tag{41}$$

We note that ι is always positive, and thus, nontrivial free-oscillation amplitudes occur only when $\nu > 0$ and $\nu^2 \geq \iota$. These conditions demand that:

$$\Lambda_n^2 < \frac{4\omega_0\sigma_e}{27\Gamma_{nnnn}}, \frac{\Gamma_{nnnn}\Lambda_n^2}{\omega_0}\left(\sigma_e - \frac{63\Gamma_{nnnn}\Lambda_n^2}{8\omega_0}\right) - 2\mu_{ne}^2 \geq 0. \tag{42}$$

is follows that Γ_{nnnn} and σ_e must have the same sign.

It follows from Equation (42) that, for a given Λ_n, nontrivial solutions can exist only if:

$$\Gamma_{nnnn}\sigma_e \geq \frac{2\mu_{ne}^2\omega_0}{\Lambda_n^2} + \frac{63\Gamma_{nnnn}\Lambda_n^2}{8\omega_0} \tag{43}$$

while for a given σ_e, nontrivial solutions can exist only if:

$$\frac{\sigma_e}{\mu_{ne}} - \left(\frac{\sigma_e^2}{\mu_{ne}^2} - 63 \right)^{1/2} \leq \frac{63\Gamma_{nnnn}\Lambda_n^2}{4\omega_0\mu_{ne}} \leq \frac{\sigma_e}{\mu_{ne}} + \left(\frac{\sigma_e^2}{\mu_{ne}^2} - 63 \right)^{1/2}. \tag{44}$$

In the Λ_n-σ_e/μ_{ne}-plane, the boundary of the region where nontrivial solutions can exist is given by:

$$\frac{63\Gamma_{nnnn}\Lambda_n^2}{4\omega_0\mu_{ne}} = \frac{\sigma_e}{\mu_{ne}} \pm \left(\frac{\sigma_e^2}{\mu_{ne}^2} - 63 \right)^{1/2} \tag{45}$$

For $\Gamma_{nnnn} > 0$, Figure 8 shows the regions where the subharmonic response exists. Figures 9 and 10 show the amplitude-frequency curve and the response-excitation amplitude curve of the subharmonic resonance of different time delay and control gain. We note that there is no jump phenomenon in this case.
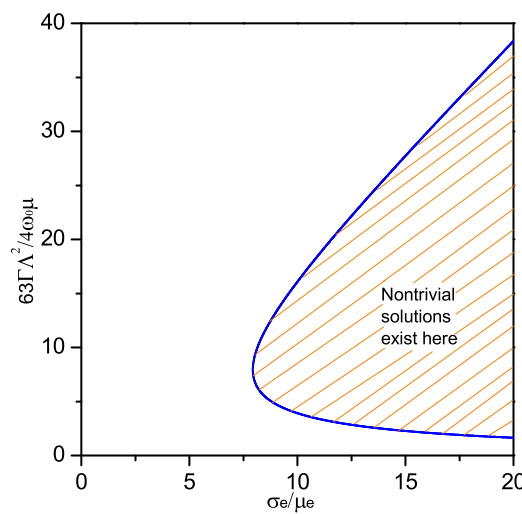

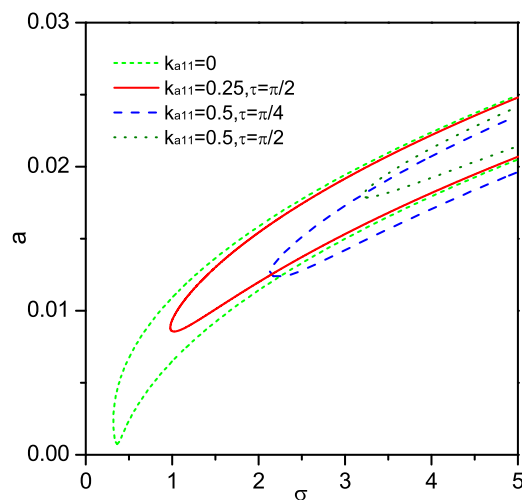**Figure 8.** Regions where the subharmonic response exists.

Figure 9. The amplitude-frequency curve of the subharmonic resonance.

Can be seen from Figure 10, as k_{a11} increases, the resonance regions decrease obviously, but as τ increases, those are on the contrary. As excitation amplitude increases, the resonance curve moves to the right, the resonance regions of the system expand, and the vibration amplitude increases. The subharmonic resonance regions of the system are very sensitive to external excitation amplitude.

It is worth noting that the amplitude can be effectively suppressed by adjusting the control gain k_{a11} and time delay.
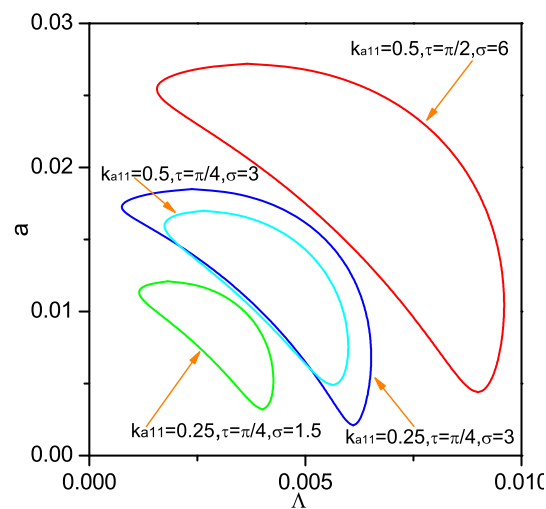

Figure 10. The response-excitation amplitude curve of the subharmonic resonance.

5. Conclusions

In this paper, we study the control effect of time-delayed displacement feedback control on the superharmonic and subharmonic resonance response of the elastic beam. The first-order approximate solutions of the superharmonic and subharmonic resonance containing the control parameters are obtained. The response curves of the external excitation amplitude f, the control gain k, and the time delay τ are presented. The results show that the vibration of the beam can be effectively suppressed by using the time-delayed displacement feedback control. Adjusting the control gain and time delay can avoid the resonance region and unstable solutions. Hence, the time-delayed displacement feedback is an effective control strategy to control the vibration of the system.

Author Contributions: All the authors actively contributed to the research described herein. J.P. conceived the idea of this research and wrote the manuscript, M.X. and L.L. implemented the various mathematical expressions and analyzed, and H.S. and X.W. revised the manuscript.

Conflicts of Interest: The authors declare no conflict of interest. .

References

1. Ma, J.J.; Liu, F.J.; Nie, M.Q.; Wang, J.B. Nonlinear free vibration of a beam on Winkler foundation with consideration of soil mass motion of finite depth. *Nonlinear Dyn.* **2018**, *92*, 429–441. [CrossRef]
2. Ma, J.J.; Gao, X.J.; Liu, F.J. Nonlinear lateral vibrations and two-to-one resonant responses of a single pile with soil-structure interaction. *Meccanica* **2017**, *52*, 3549–3562. [CrossRef]
3. Zhong, X.G.; Peng, X.; Yan, S.K.; Shen, M.Y.; Zhai, Y.Y. Assessment of the feasibility of detecting concrete cracks in images acquired by unmanned aerial vehicles. *Autom. Constr.* **2018**, *89*, 49–57. [CrossRef]
4. Wang, W.X.; Wang, X.Y.; Hua, X.G.; Song, G.B.; Chen, Z.Q. Vibration control of vortex-induced vibrations of a bridge deck by a single-side pounding tuned mass damper. *Eng. Struct.* **2018**, *173*, 61–75. [CrossRef]
5. Wang, W.X.; Hua, X.G.; Wang, X.Y.; Chen, Z.Q.; Song, G.B. Optimum design of a novel pounding tuned mass damper under harmonic excitation. *Smart Mater. Struct.* **2017**, *26*, 055024. [CrossRef]
6. Wen, Q.; Hua, X.G.; Lei, X.; Chen, Z.Q.; Niu, H.W. Experimental study of wake-induced instability of coupled parallel hanger ropes for suspension bridges. *Eng. Struct.* **2018**, *167*, 175–187. [CrossRef]

7.　Wen, Q.; Hua, X.G.; Chen, Z.Q.; Niu, H.W.; Wang, X.Y. AMD-Based Random Decrement Technique for Modal Identification of Structures with Close Modes. *J. Aerosp. Eng.* **2018**, *5*, 04018057. [CrossRef]

8.　Lin, W.; Song, G.B.; Chen, S.H. PTMD control on a benchmark tv tower under earthquake and wind load excitations. *Appl. Sci.* **2017**, *7*, 425. [CrossRef]

9.　Sun, H.; Zuo, L.; Wang, X.; Peng, J.; Wang, W. Exact H2 optimal solutions to inerter-based isolation systems for building structures. *Struct. Control Health Monit.* **2019**, e2357. [CrossRef]

10.　Qian, H.; Li, H.N.; Song, G.B. Experimental investigations of building structure with a superelastic shape memory alloy friction damper subject to seismic loads. *Smart Mater. Struct.* **2016**, *25*, 125026. [CrossRef]

11.　Lin, W.; Lin, Y.L.; Song, G.B.; Li, J. Multiple Pounding Tuned Mass Damper (MPTMD) control on benchmark tower subjected to earthquake excitations. *Earthq. Struct.* **2016**, *11*, 1123–1141. [CrossRef]

12.　Li, H.N.; Zhang, P.; Song, G.B.; Patil, D.; Mo, Y.L. Robustness study of the pounding tuned mass damper for vibration control of subsea jumpers. *Smart Mater. Struct.* **2015**, *24*, 095001. [CrossRef]

13.　Wang, W.X.; Hua, X.G.; Wang, X.Y.; Wu, J.L.; Sun, H.X.; Song, G.B. Mechanical behavior of magnetorheological dampers after long-term operation in a cable vibration control system. *Struct. Control Health* **2019**, *26*, e2280. [CrossRef]

14.　Yu, Y.; Li, L.Y.; Leng, X.Z.; Song, G.B.; Liu, Z.Q.; Ou, J.P. A wireless decentralized control experimental platform for vibration control of civil structures. *Smart. Struct. Syst.* **2017**, *19*, 47–56. [CrossRef]

15.　Wang, H.; Li, L.Y.; Song, G.B.; Dabney, J.B. Harman, T.L. A new approach to deal with sensor errors in structural controls with MR damper. *Smart. Struct. Syst.* **2015**, *16*, 329–345. [CrossRef]

16.　Shivashankar, P.; Kandagal, S.B. Characterization of elastic and electromechanical nonlinearities in piezoceramic plate actuators from vibrations of a piezoelectric-beam. *Mech. Syst. Signal Process.* **2019**, *116*, 624–640. [CrossRef]

17.　Zhou, Z.H.; Ni, Y.W.; Zhu, S.B.; Tong, Z.Z.; Sun, J.B; Xu, X.S. An accurate and straightforward approach to thermo-electro-mechanical vibration of piezoelectric fiber-reinforced composite cylindrical shells. *Compos. Struct.* **2019**, *207*, 292–303. [CrossRef]

18.　Bricault, C.; Pezerat, C.; Collet, M.; Pyski, A.; Perrard, P.; Matten, G.; Romero-Garcia, V. Multimodal reduction of acoustic radiation of thin plates by using a single piezoelectric patch with a negative capacitance shunt. *Appl. Acoust.* **2019**, *145*, 320–327. [CrossRef]

19.　Feng, Q.; Liang, Y.B.; Song, G.B. Real-time monitoring of early-age concrete strength using piezoceramic-based smart aggregates. *J. Aerosp. Eng.* **2019**, *32*, 04018115. [CrossRef]

20.　Lim, Y.Y.; Tang, Z.S.; Smith, S.T. Piezoelectric-based monitoring of the curing of structural adhesives: A novel experimental study. *Smart Mater. Struct.* **2019**, *28*, 107532. [CrossRef]

21.　Jiang, T.Y.; Zhang, Y.W.; Wang, L.; Zhang, L.; Song, G.B. Monitoring fatigue damage of modular bridge expansion joints using piezoceramic transducers. *Sensors* **2018**, *18*, 3973. [CrossRef]

22.　Chen, M.F.; Chen, H.L.; Ma, X.L.; Jin, G.Y.; Ye, T.G.; Zhang, Y.T.; Liu, Z.G. The isogeometric free vibration and transient response of functionally graded piezoelectric curved beam with elastic restraints. *Results Phys.* **2018**, *11*, 71225. [CrossRef]

23.　Przybylski, J.; Gasiorski, G. Nonlinear vibrations of elastic beam with piezoelectric actuators. *J. Sound Vib.* **2018**, *437*, 150–165. [CrossRef]

24.　Ling, M.X.; Cao, J.Y.; Li, Q.S.; Zhuang, J. Design, pseudostatic model, and pvdf-based motion sensing of a piezo-actuated XYZ flexure manipulator. *IEEE ASME Trans. Mech.* **2018**, *23*, 2837–2848. [CrossRef]

25.　Presas, A.; Luo, Y.; Wang, Z.; Valentin, D.; Egusquiza, M. A Review of PZT Patches Applications in Submerged Systems. *Sensors* **2018**, *18*, 2251. [CrossRef]

26.　Wang, T.; Wei, D.L.; Shao, J.H.; Li, Y.R.; Song, G.B. Structural stress monitoring based on piezoelectric impedance frequency shift. *J. Aerosp. Eng.* **2018**, *31*, 8. [CrossRef]

27.　Olgac, N.; Holm-Hansen, B. A Novel Active Vibration Absorption Technique: Delayed Resonator. *J. Sound Vib.* **1994**, *176*, 93–104. [CrossRef]

28.　Vyhlal, T.; Olgac, N.; Kucera, V. Delayed resonator with acceleration feedback-Complete stability analysis by spectral methods and vibration absorber. *J. Sound Vib.* **2014**, *333*, 6781–6795. [CrossRef]

29.　Kammer, A.S.; Olgac, N. Delayed-feedback vibration absorbers to enhance energy harvesting. *J. Sound Vib.* **2016**, *363*, 54–67. [CrossRef]

30.　Ma, J.Z.; Zhang, S.J.; Luan, M.Y.; Wang, J.P. Experimental investigation on delay time phenomenon in rotating detonation engine. *Aerosp. Sci. Technol.* **2019**, *88*, 395–404. [CrossRef]

31. Yan, G.; Fang, M.X.; Xu, J. Analysis and experiment of time-delayed optimal control for vehicle suspension system. *J. Sound Vib.* **2019**, *446*, 144–158. [CrossRef]

32. Zheng, P.X.; Long, X.H. Active control of time-delay in cutting vibration. *Theor. Appl. Mech. Lett.* **2013**, *3*, 063003. [CrossRef]

33. Salehi, H.; Das, S.; Chakrabartty, S.; Biswas, S.; Burgueño R. An algorithmic framework for reconstruction of time-delayed and incomplete binary signals from an energy-lean structural health monitoring system. *Eng. Struct.* **2019**, *180*, 603–620. [CrossRef]

34. Chen, L.X.; Cai, G.P. Design method of multiple time-delay controller for active structural vibration control. *Appl. Math. Mech. Engl.* **2009**, *30*, 1405–1414. [CrossRef]

35. Hu, H.Y.; Wang, Z.H. *Dynamics of Controlled Mechanical Systems with Delayed Feedback*; Springer: Berlin/Heidelbeg, Germany, 2002.

36. Wang, Z.H.; Hu, H.Y. Stabilization of vibration systems via delayed state difference feedback. *J. Sound Vib.* **2006**, *296*, 117–129. [CrossRef]

37. Masoud, Z.; Daqaq, M.F.; Nayfeh, N.H. Pendulation reduction of small telescopic cranes. *J. Vib. Control* **2004**, *10*, 1167–1179.

38. Daqaq, M.F.; Alhazza, K.A.; Arafat, H.N. Non-linear vibrations of cantilever beams with feedback delays. *Int. J. Nonlinear Mech.* **2008**, *43*, 962–978. [CrossRef]

39. Qian, C.Z.; Tang, J.S. A time delay control for a nonlinear dynamic beam under moving load. *J. Sound Vib.* **2008**, *309*, 1–8. [CrossRef]

40. Xu, J.; Yu, P. Delay-induced bifurcations in a nonautonomous system with delayed velocity feedbacks. *Int. J. Bifurc. Chaos* **2004**, *14*, 2777–2798. [CrossRef]

41. Kalmar-Nagy, T.; Stepan, G.; Moon, F.C. Subcritical Hopf bifurcation in the delay equation model for machine tool vibrations. *Nonlinear Dyn.* **2001**, *26*, 121–142. [CrossRef]

42. Peng, J.; Wang, L.H.; Zhao, Y.Y.; Zhao, Y.B. Bifurcation analysis in active control system with time delay feedback. *Appl. Math. Comput.* **2013**, *219*, 10073–10081. [CrossRef]

43. Li, X.Y.; Ji, J.C.; Hansen, C.H.; Tan, C.X. The response of a Duffing-van der Pol oscillator under delayed feedback control. *J. Sound Vib.* **2006**, *291*, 644–655. [CrossRef]

44. Jin, Y.F.; Hu, H.Y. Stabilization of traffic flow in optimal velocity model via delayed-feedback control. *Commun. Nonlinear Sci.* **2013**, *18*, 1027–1034. [CrossRef]

45. Omidi, E.; Mahmoodi, S.N. Sensitivity analysis of the nonlinear integral positive position feedback and integral resonant controllers on vibration suppression of nonlinear oscillatory systems. *Commun. Nonlinear Sci.* **2015**, *22*, 149–166. [CrossRef]

46. Omidi, E.; Mahmoodi, S.N. Nonlinear vibration suppression of flexible structures using nonlinear modified positive position feedback approach. *Nonlinear Dyn.* **2015**, *79*, 835–849. [CrossRef]

47. El-Ganaini, W.A.; Saeed, N.A.; Eissa, M. Positive position feedback (PPF) controller for suppression of nonlinear system vibration. *Nonlinear Dyn.* **2013**, *72*, 517–537. [CrossRef]

48. Warminski, J.; Bochenski, M.; Jarzyna, W.; Filipek, P.; Augustyniak, M. Active suppression of nonlinear composite beam vibrations by selected control algorithms. *Commun. Nonlinear Sci.* **2011**, *16*, 2237–2248. [CrossRef]

49. Belhaq, M.; Ghouli, Z.; Hamdi, M. Energy harvesting in a Mathieu-van der Pol-Duffing MEMS device using time delay. *Nonlinear Dyn.* **2018**, *94*, 2537–2546. [CrossRef]

50. Hamdi, M.; Belhaq, M. Quasi-periodic vibrations in a delayed van der Pol oscillator with time-periodic delay amplitude. *J. Vib. Control* **2018**, *24*, 5726–5734. [CrossRef]

51. Zhang, X.; Xu, J.; Ji, J. Modelling and tuning for a time-delayed vibration absorber with friction. *J. Sound Vib.* **2018**, *424*, 137–157. [CrossRef]

52. Ji, J.C.; Zhou, J. Coexistence of two families of sub-harmonic resonances in a time-delayed nonlinear system at different forcing frequencies. *Mech. Syst. Signal Process.* **2017**, *93*, 151–163. [CrossRef]

53. Ji, J.C.; Brown, T. Periodic and Chaotic Motion of a Time-Delayed Nonlinear System under Two Coexisting Families of Additive Resonances. *Int. J. Bifurc. Chaos* **2017**, *27*, 1750066. [CrossRef]

54. Nayfeh, A.H. *Linear and Nonlinear Structure Mechanics*; Wiley Interscience: New York, NY, USA, 2004.

55. Ma, J.J.; Liu, F.J.; Gao, X.J.; Nie, M.Q. Buckling and free vibration of a single pile considering the effect of soil-structure interaction. *Int. J. Struct. Stab. Dyn.* **2017**, *18*, 1850061. [CrossRef]

56. Ma, J.J.; Peng, J.; Gao, X.J.; Xie, L. Effect of soil-structure interaction on the nonlinear response of an inextensional beam on elastic foundation. *Arch. Appl. Mech.* **2014**, *85*, 273–285. [CrossRef]

57. Nayfeh, A.H.; Mook, D.T. *Nonlinear Oscillations*; Wiley: Hoboken, NJ, USA, 1979.